

Quantitative Determination of Threading in Rotaxanated Polymers by Diffusion-Ordered NMR Spectroscopy

Tiejun Zhao and Haskell W. Beckham*

Polymer Education and Research Center, School of Textile and Fiber Engineering,
Georgia Institute of Technology, Atlanta, Georgia 30332-0295

Harry W. Gibson

Department of Chemistry, Virginia Polytechnic Institute & State University,
Blacksburg, Virginia 24061

Received December 12, 2002; Revised Manuscript Received April 10, 2003

ABSTRACT: Two-dimensional diffusion-ordered NMR spectroscopy (DOSY) was used to examine a rotaxanated polymer and its blends with unthreaded macrocycles. The threaded macrocycles exhibit self-diffusion coefficients similar to those of the polymer, while the diffusion coefficients for the unthreaded macrocycles are much larger. For poly[(styrene)-*rotaxa*-(30-crown-10)], the method provided definitive proof that the 30-crown-10 is threaded; for blends, the method allowed quantitative determination of the threaded-macrocycle fraction. The DOSY technique is particularly useful for those rotaxanated polymers in which weakly interacting macrocycle and polymer offer no other detectable spectroscopic signature. Threading can be proven, and the fraction of threaded macrocycles can be determined.

Introduction

Molecular architectures that consist of cyclic molecules threaded onto linear polymer segments are called *polyrotaxanes* when bulky end groups block dethreading of the cyclic component and *polypseudorotaxanes* when blocking groups are not present.^{1,2} We generally refer to both types as *rotaxanated* polymers. Syntheses of rotaxanated polymers are typically followed by experiments to determine whether the macrocycles are threaded or not. In some cases, threaded macrocycles cause or experience changes in local electronic structure that are detectable by various spectroscopic techniques. For example, changes in NMR chemical shifts of macrocycles are observed when there exists hydrogen bonding, charge transfer, or dipolar coupling interactions with the backbone.^{3–9}

However, many rotaxanated structures have been prepared for which threading is not accompanied by changes in the local electronic structure. This is often the case for rotaxanated materials with no specific interactions between macrocycle and linear polymer. For example, some polyrotaxanes based on aliphatic crown ethers do not exhibit NMR chemical shift changes from those of their respective unthreaded components.^{10–13} Many of these threaded architectures are created by polymerization in macrocycle solvents or cosolvents. Following polymerization, the product contains both threaded and unthreaded macrocycles. It is dissolved in a good solvent for both components and then precipitated in a selective solvent for the unthreaded macrocycle. The macrocycle content of the product can be followed spectroscopically. The dissolution/precipitation procedure is repeated until the macrocycle content becomes constant. At this point it is assumed that the remaining macrocycles are threaded. However, a more direct method to determine whether the macrocycles are

threaded is desired for (1) definitive proof of threading, (2) quantification of threaded and unthreaded fraction, and (3) examination of threading/dethreading kinetics in polypseudorotaxanes.

Self-diffusion depends on molecular size. Since macrocycles are typically much smaller than the polymers on which they are threaded, the two components of a rotaxanated polymer should exhibit vastly different intrinsic self-diffusion behavior. When the two components are threaded, the macrocycle self-diffusion should be governed by the self-diffusion of the polymer. Diffusion-ordered NMR spectroscopy (DOSY)^{14–18} can be used to correlate diffusion coefficients with molecular structure via chemical shifts. It has been successfully applied to study molecular association, which causes changes in self-diffusion coefficients; the association constants of several guest–host complexes, such as cyclodextrin and various small molecules, have been determined.^{19–21} In fact, DOSY has been used to study pseudorotaxane formation between α -cyclodextrin and a series of homologous α,ω -diaminoalkanes.²² The technique should be useful also for quantitative determination of threading in rotaxanated polymers.

Experimental Section

The materials chosen for this study include polystyrene (PS), 30-crown-10 (30c10), and the rotaxanated polymer (see Figure 1) consisting of these components, poly[(styrene)-*rotaxa*-(30-crown-10)] (PS-*rotaxa*-30c10). All materials were dried at 50 °C under vacuum for 2 days before use and then dissolved into CDCl₃ (Aldrich, 99.9%) at concentrations around 0.7% (w/w) for NMR analysis. Physical blends of 30c10/PS and 30c10/PS-*rotaxa*-30c10 were prepared by dissolving each component directly in CDCl₃. The PS, a commercial sample chosen because of its molecular-weight similarity to the rotaxanated polymer, was characterized by gel permeation chromatography: $M_n = 7 \times 10^4$ g/mol and $M_w = 3 \times 10^5$ g/mol. The 30c10 and PS-*rotaxa*-30c10 were prepared according to published methods.^{23,24} The PS-*rotaxa*-30c10 (molecular weight $\sim 10^4$ g/mol) contains bulky tris(*p*-*tert*-butylphenyl)methyl groups at the PS chain ends that prevent dethreading of 30c10 (see

* To whom correspondence should be addressed. E-mail: haskell.beckham@tfe.gatech.edu.

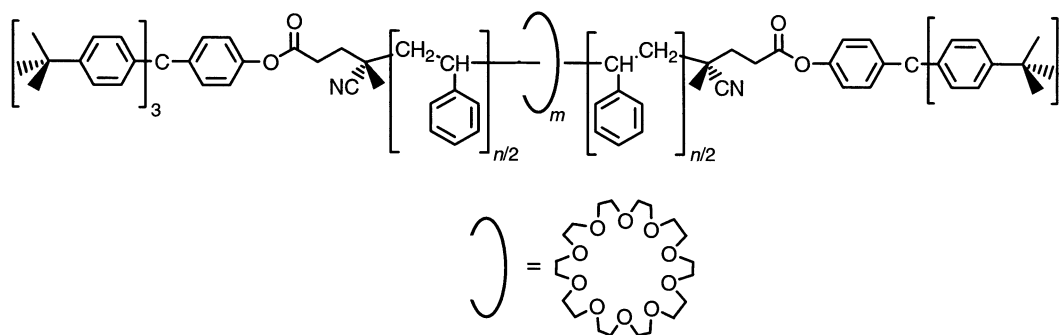


Figure 1. Structure of the rotaxanated polymer, poly[(styrene)-rotaxa-(30-crown-10)], also referred to as PS-*rotaxa*-30c10. The 30-crown-10 content of the sample used in this study is 2 wt %, corresponding to a threading ratio (m/n) of 0.005.

Figure 1). Threading of crown ethers onto non-end-blocked PS can occur.²⁴ A THF solution containing 16 wt % 42-crown-14 and 1.6 wt % PS ($M_n = 18$ kg/mol) was refluxed for a week to yield the rotaxanated PS containing 0.3 wt % 42-crown-14. However, threading is not expected to occur to any significant extent for the 30c10/PS blend prepared here due to the lower concentrations of components in solution (0.7 wt % vs 17 wt %) and the much shorter threading time (hours at 20 °C vs a week at reflux).

All NMR experiments were performed on dilute solutions in 5 mm NMR tubes at a constant temperature of 20 °C using a Bruker DRX 500 spectrometer. The DOSY experiments employed the bipolar pulse pair and longitudinal eddy current delay (BPP-LED) sequence.²⁵ Field gradient calibration was accomplished using the self-diffusion coefficient of pure water at 25 °C (2.299×10^{-9} m² s⁻¹).²⁶ The gradients were applied for 2 ms ($\delta/2$), and the diffusion time (Δ) was 80 ms. Gradient settling times were 500 μ s, and the eddy current elimination duration was 5 ms. Homospoil gradients were applied for 1 ms during the diffusion and eddy current settling durations. The gradients (g) were incremented 32 times from 1.7 to 63.0 G/cm, resulting in attenuation of the polystyrene resonances to approximately 2% of their original intensities. A total of 128 free induction decays containing 64K points were collected at each gradient amplitude. The delay between each scan was 2 s, and 120 dummy scans were applied before the first data were collected.

For molecules experiencing Brownian motion, the echo amplitude decay, $I(g)$, can be described as

$$I(g) = I(0) \int_0^\infty w(D, T_1, T_2, \delta) \exp(-kD) dD \quad (1)$$

where w is a relaxation-weighted fraction with a specific diffusion coefficient (D), spin-lattice relaxation time (T_1), and spin-spin relaxation time (T_2), measured for a given gradient duration (δ). $k = (\gamma g \delta)^2 (\Delta - \delta/3)$, where γ is the magnetogyric ratio of the nucleus under observation (proton for this research). To extract the diffusion coefficient distribution, an inverse Laplace transform (ILT) is carried out along the first dimension following Fourier transformation along the chemical shift dimension. The ILT was performed using routines that are part of the Bruker XWIN-NMR package. These routines are based on the CONTIN algorithm.^{27,28} The data were also processed by fitting to a bimodal exponential using MATLAB.

Spin-spin (T_2) relaxation times were determined using a standard Carr-Purcell-Meiboom-Gill (CPMG) sequence with 21 different delays from 0.03 to 4.5 s, 16 scans, and a 6 s recovery time. Spin-lattice (T_1) relaxation times were measured using an inversion-recovery pulse sequence with 16 different delays from 0.01 to 10 s, 16 scans, and a 10 s recovery time.

Results and Discussion

The PS-*rotaxa*-30c10 (Figure 1) used in this study contains 2 wt % 30c10, of which 100% is threaded. By mixing the PS-*rotaxa*-30c10 with 4 and 10 wt % un-

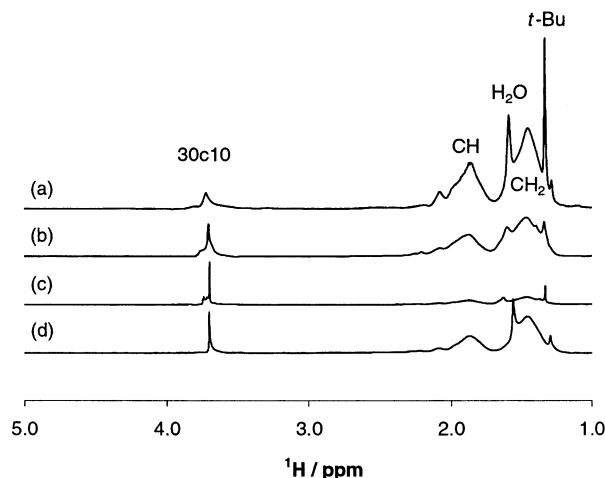


Figure 2. ¹H NMR spectra for (a) PS-*rotaxa*-30c10 (2 wt % 30c10, 100% of the crowns are threaded), (b) a (4/96, w/w) 30c10/PS-*rotaxa*-30c10 physical blend in which 32% of the crowns are threaded, (c) a (10/90, w/w) 30c10/PS-*rotaxa*-30c10 physical blend in which 15% of the crowns are threaded, and (d) a (2/98, w/w) 30c10/PS physical blend (0% of the crowns are threaded).

threaded 30c10, blends were prepared in which 32% of the macrocycles are threaded and 15% of the macrocycles are threaded, respectively. A 30c10/PS physical blend was also prepared with 2 wt % 30c10, of which 0% is threaded. The ¹H NMR spectra of these four samples (phenyl proton region not shown) are presented in Figure 2 and appear similar. From top to bottom, the spectra represent materials with decreasing fraction of threaded macrocycle. In addition to the peaks due to the protons of the polystyrene repeat unit, peaks also exist for water (1.58 ppm), *tert*-butyl-containing end groups (1.33 ppm), and the solvent (spectral region not shown).²⁴ The small narrow peak at 1.29 ppm is due to an initiator fragment or impurity. The H₂O chemical shift in the 30c10/PS physical blend (Figure 2d) is slightly upfield from that for the threaded samples, indicating the 30c10/water interaction may be influenced by the physical state of the 30c10. The crown, whether or not it is threaded, appears as a peak near 3.7 ppm. No significant change in the 30c10 chemical shift occurs upon threading since no strong chemical interactions exist between 30-crown-10 and polystyrene. However, the peak for the threaded 30-crown-10 (Figure 2a) is noticeably broader than the peak for the unthreaded 30-crown-10 (Figure 2d). For the physical blends, the 30c10 peak contains a larger narrow component as the fraction of unthreaded macrocycle increases. The broadening observed for the threaded 30-

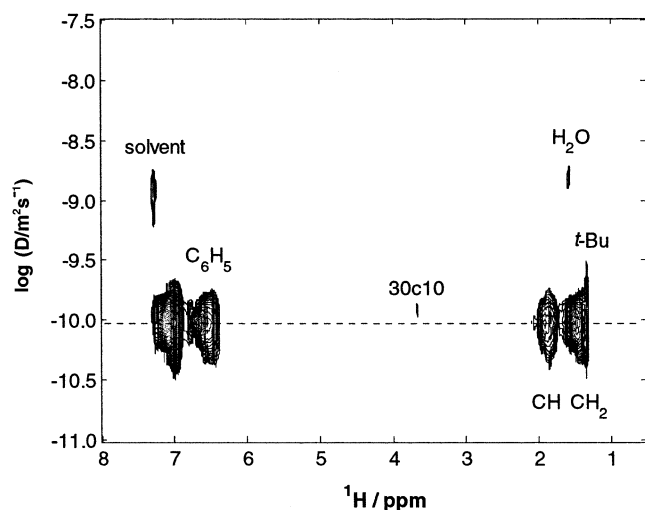


Figure 3. 2D DOSY spectrum of poly[(styrene)-rotaxa-(30-crown-10)]. All of the 30-crown-10 is threaded in this sample and cannot dethread due to bulky *tert*-butyl-containing end groups (labeled in spectrum as *t*-Bu).²⁴ $T = 20\text{ }^{\circ}\text{C}$, 0.7 wt % in CDCl_3 .

crown-10 is due to a decrease in dynamic conformational averaging; for an unthreaded macrocycle, such averaging reduces chemical shift dispersion and residual dipolar couplings to yield a narrow NMR peak.

While a broad 30c10 NMR peak provides evidence that the 30c10 is threaded, it is not definitive proof. Peak broadening in NMR spectra of polymers can often be related to overall solution viscosity. Thus, for samples in which both threaded and unthreaded macrocycles exist, it may not be straightforward to quantify their relative proportions by deconvolution of the NMR peak into broad and narrow components, respectively (see Figure 2). An alternative approach is diffusion-ordered NMR spectroscopy (DOSY). The DOSY spectrum of the pure PS-rotaxa-30c10 is shown in Figure 3 as a 2D plot of self-diffusion coefficients vs proton chemical shift. The self-diffusion coefficients (D) of the PS backbone (CH and CH_2) and side groups (C_6H_5) are similar ($D \sim 10^{-10} \text{ m}^2 \text{ s}^{-1}$) to each other and agree with previously reported D values for random-coil polystyrene in dilute solution.²⁹ The threaded 30c10 exhibits a diffusion coefficient that is slightly larger than the average, but within the diffusion coefficient distribution of the polystyrene resonances. The threaded 30c10 and PS backbone of this rotaxanated polymer are self-diffusing as single entities in solution.

The 2D DOSY spectrum of a physical blend of polystyrene and 30-crown-10 was also measured (not shown). The PS backbone and side-chain diffusion coefficients are equivalent to each other and similar to those of the rotaxanated PS shown in Figure 3, which is expected due to the similarity in molecular weights ($\sim 10^4 \text{ g/mol}$). However, as opposed to the threaded 30c10 in the rotaxanated PS, the unthreaded 30c10 in the 30c10/PS physical blend exhibits much larger diffusion coefficients than the PS, as might be expected on the basis of their differences in molecular sizes. The unthreaded 30c10 also exhibits a larger diffusion coefficient [$\log(D/\text{m}^2 \text{ s}^{-1}) = -9.4$] than the threaded 30c10 [$\log(D/\text{m}^2 \text{ s}^{-1}) = -9.9$] of PS-rotaxa-30c10 shown in Figure 3.

Thus, threaded and unthreaded macrocycles should be distinguishable using such spectra. To test this hypothesis, 2D DOSY spectra were measured on physi-

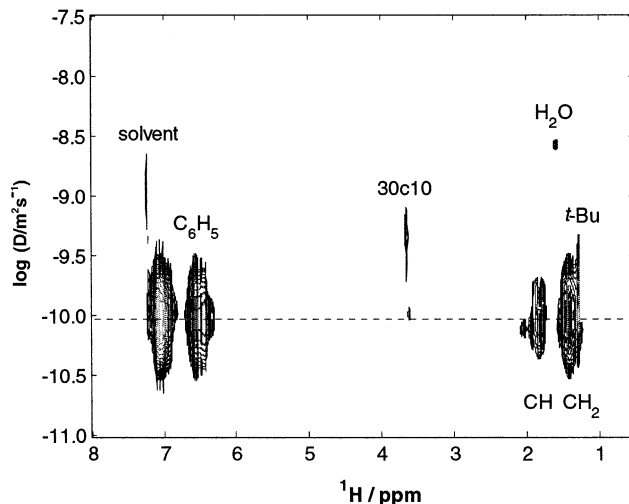


Figure 4. 2D DOSY spectrum of a 30c10/PS-rotaxa-30c10 (4/96, w/w) physical blend. Of the total 30c10 content, 32% are threaded. Note the two peaks along the diffusion axis for the threaded (near the horizontal dashed line) and unthreaded 30c10. $T = 20\text{ }^{\circ}\text{C}$, 0.7 wt % in CDCl_3 .

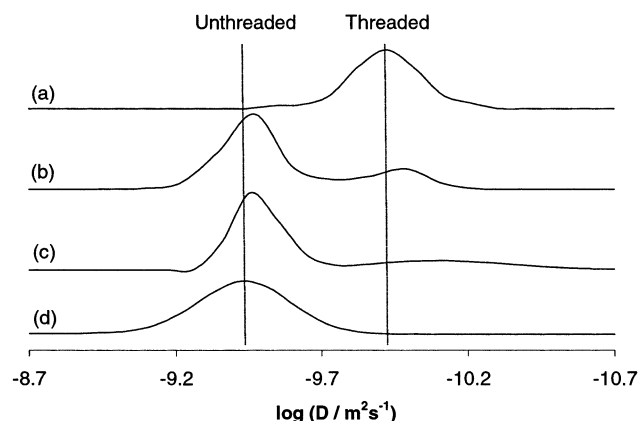


Figure 5. Diffusion coefficient distributions obtained by extracting slices at 3.7 ppm (30c10) along the diffusion dimension of 2D DOSY spectra for (a) PS-rotaxa-30c10 (2 wt % 30c10, 100% of the crowns are threaded), (b) a (4/96, w/w) 30c10/PS-rotaxa-30c10 physical blend in which 32% of the crowns are threaded, (c) a (10/90, w/w) 30c10/PS-rotaxa-30c10 physical blend in which 15% of the crowns are threaded, and (d) a (2/98, w/w) 30c10/PS physical blend (0% of the crowns are threaded).

cal blends of the rotaxanated PS with unthreaded 30-crown-10; these samples contained known concentrations of threaded and unthreaded macrocycles. The DOSY spectrum of the physical blend made with 4 wt % unthreaded 30c10 (32% of the total crown content is threaded) is shown in Figure 4 and appears quite similar to the spectrum of the pure rotaxanated sample shown in Figure 3. One important difference is the presence of two separate peaks along the diffusion axis at 3.7 ppm, representing the threaded and unthreaded crown. The line widths along the diffusion dimension are related to the choice of contour levels in these 2D plots. The data are perhaps best presented in a 1D slice taken along the diffusion dimension at 3.7 ppm. This slice is displayed in Figure 5 for the two DOSY spectra shown above, along with the slices from the 2D DOSY spectra of the 30c10/PS and 30c10/PS-rotaxa-30c10 (10/90, w/w) physical blends. The threaded crown exhibits a smaller diffusion coefficient than the unthreaded crown. Two peaks, corresponding to threaded and un-

Table 1. NMR Relaxation Times for 30c10

sample	T_1/s	T_2/s
30c10/PS	2.7	1.5
PS- <i>rotaxa</i> -30c10	2.2	1.0

Table 2. Fraction of Threaded 30c10 in 30c10/PS-*rotaxa*-30c10 Physical Blends

	30c10/PS- <i>rotaxa</i> -30c10 blend/%	
	4/96 (w/w)	10/90 (w/w)
actual ^a	32.4	15.3
CONTIN	29	11
bimodal model	35	14

^a Actual values were calculated from the weight fraction of 30c10 and PS-*rotaxa*-30c10 in each blend and the fact that there are 2 wt % threaded 30c10 in the PS-*rotaxa*-30c10.

threaded 30c10, are observed for both 30c10/PS-*rotaxa*-30c10 physical blends. For the sample in which 15% of the 30c10 is threaded (Figure 5c), the threaded 30c10 is represented by a relatively broad distribution.³⁰

To quantify the fraction of threaded vs unthreaded macrocycles in a given sample, the relative peak intensities shown in Figure 5 should depend only on the amount of each component. However, these peak intensities also depend on NMR relaxation times (see eq 1). If the relaxation weighting of the peaks is similar, or corrected, the relative peak intensities should be quantitative. For high-molecular-weight polymers, relaxation rates are typically governed by segmental motions. It was suggested that the 30-crown-10 segmental motions are affected by threading as evidenced by the NMR peak broadening (see Figure 2). Thus, differential relaxation weighting for the threaded and unthreaded 30c10 signals could preclude quantitative analysis. Relaxation times were therefore measured for the rotaxanated PS and the 30c10/PS physical blend. The T_1 and T_2 for the threaded and unthreaded 30c10 are shown in Table 1. Shorter T_2 for the threaded 30c10 is consistent with a broadened line compared to the unthreaded 30c10. Assuming the relaxation weighting was sufficiently similar, the peaks were integrated to estimate the relative fraction of threaded crown in each sample. The results, shown in Table 2, are close to the actual values for the two blends of 30c10 with PS-*rotaxa*-30c10. Some of the deviation from the actual values may be due to the different relaxation rates of a threaded vs unthreaded macrocycle. For macrocycles larger than 30-crown-10, relaxation rate differences are expected to diminish as threading-induced perturbations to segmental dynamics become increasingly insignificant.

In Figures 3 and 4, peaks exist for the NMR solvent (CDCl_3) and H_2O , which exhibit significantly larger diffusion coefficients than the polymer due to their much smaller molecular sizes. The $\log(D/\text{m}^2\text{s}^{-1})$ for pure water is -8.6 , which is very close to the values observed in the DOSY spectra of Figures 3 and 4. For all other samples, the water diffusion coefficient was also similar or slightly smaller than that of pure water. Furthermore, while small molecules such as water and solvent might be expected to exhibit discrete diffusion coefficients, they have rather broad D distributions in the 2D DOSY spectra. Some of the broadening and decreased D is due to the various associations of solvent, water, macromolecule, and macrocycle, while some of it is an artifact of the data processing scheme. Overlapping signals in the chemical shift dimension lead to impure decay curves and diffusion coefficients that

Table 3. Self-Diffusion Coefficients of 30c10 in Blends with PS

threaded 30c10 fraction/%	CONTIN ^a		bimodal	
	$\log(D_t/\text{m}^2\text{s}^{-1})$	$\log(D_u/\text{m}^2\text{s}^{-1})$	$\log(D_t/\text{m}^2\text{s}^{-1})$	$\log(D_u/\text{m}^2\text{s}^{-1})$
0		-9.42		-9.36
15	-10.0	-9.44	-9.73	-9.32
32	-9.97	-9.47	-9.84	-9.30
100	-9.90		-9.90	

^a Peak values of diffusion coefficient distribution are used. D_t = diffusion coefficient for threaded 30c10; D_u = diffusion coefficient for unthreaded 30c10.

represent some average of the components, and the CONTIN algorithm applied here includes a smoothing feature that often overbroadens peaks for monodisperse components.³⁰

A number of processing schemes exist in addition to using the CONTIN analysis to calculate diffusion coefficients from DOSY data.³¹ In fact, when the number of components in a sample is known, the relative proportions of each may be calculated with greater precision using one of the other methods.³² Such is the case for the physical blends containing threaded and unthreaded macrocycles. Following collection of a DOSY data set, Fourier transformation along the chemical shift dimension yields a stacked plot of spectra for different gradient strengths. The intensity of the 30c10 peak can then be plotted vs k (see eq 1) to provide a diffusion decay curve. The diffusion decay curve is then fit to a biexponential expression:

$$I(g)/I(0) = w_u \exp(-kD_u) + w_t \exp(-kD_t) \quad (2)$$

where w_u and w_t are the weight fractions of unthreaded and threaded 30c10, respectively ($w_u + w_t = 1$). In this case, the fraction of unthreaded and threaded 30c10 can be determined by simple least-squares fitting. The diffusion decay curves for the PS-*rotaxa*-30c10 (100% threaded 30c10) and the 30c10/PS physical blend (0% threaded) were assumed to be monoexponential (w_u or $w_t = 0$). Equation 2 was used to fit the decay curves for the 30c10/PS-*rotaxa*-30c10 physical blends. The fitting results are listed in Tables 2 and 3 along with results obtained using the CONTIN analysis from the DOSY experiment. Fitting the data to a biexponential gave values similar to those obtained using the inverse Laplace transform.

In Figure 3, it was noted that the 30c10 of the rotaxanated PS exhibits a diffusion coefficient that is slightly larger, but within the diffusion coefficient distributions of the PS resonances. The faster-than-average diffusion behavior of the noncovalently bound macrocycles has also been observed for a rotaxanated polymer prepared from cyclic dimethylsiloxanes threaded onto poly(methyl methacrylate).³³ A related observation is the slightly larger diffusion coefficients for the polymer chain ends, signified by the *t*-Bu peaks in Figures 3 and 4. Faster apparent chain-end diffusion has been noted before and recognized as a consequence of the higher concentration of the end groups on shorter chains of a polydisperse sample.³⁴ Thus, the faster apparent diffusion behavior observed for threaded macrocycles simply indicates the macrocycles exist on the smaller chains of these polydisperse samples. These heterogeneous rotaxanated polymers have no enthalpic driving force for threading and are prepared by trapping the macrocycles on the backbones during polymeriza-

tion. Even if macrocycles are soluble in liquid monomers, phase separation can occur as polymer chains form, after which time no more threading takes place. In such cases, since the driving force for phase separation increases as molecular weights increase, macrocycles are more likely to be trapped on the chains that terminate earlier in the polymerization.

Threading of non-end-blocked polymers can occur and has been reported.^{4,24,35} For polypseudorotaxanes, macrocycles can dethread due to the absence of bulky blocking groups at the chain ends; for polymers threaded with very large macrocycles, end blocking to prevent dethreading may be impractical.³³ DOSY can be used to follow these threading and dethreading processes. If the threading/dethreading is slower than the time required to measure the DOSY spectrum, then threading/dethreading kinetics may be determined. Such experiments should be helpful in efforts to improve threading efficiencies, design processing strategies, or determine whether end blocking is necessary for processing of rotaxanated polymers.³³

Summary

2D DOSY NMR is a useful technique for proof of threading in rotaxanated polymers if diffusion coefficients of the unthreaded backbone and macrocycle are sufficiently different. This method is especially valuable when threading does not lead to easily measurable changes in standard spectra. While GPC has been used to indicate proof of threading,³⁶ peak overlap has often impeded quantification.^{3,4,24} The diffusion coefficient distributions for the macrocycle can be integrated to determine threaded fraction, as long as the relative NMR relaxation weighting of threaded and unthreaded components is similar or corrected. An alternative data processing scheme to the use of the inverse Laplace transform is to fit the diffusion decay curves to a biexponential since samples consist of two components, threaded and unthreaded macrocycles.

Acknowledgment. This work was supported by the National Science Foundation (DMR-0072876 for H.W.B. and DMR-0097126 for H.W.G.). Dr. Johannes Leisen is gratefully acknowledged for ongoing discussions and careful reading of the manuscript. Invaluable instrumentation support was provided by Dr. Leslie Gelbaum of the Georgia Tech NMR Center. The rotaxanated polystyrene was prepared at Virginia Tech by Sang-Hun Lee.

References and Notes

- (a) Gibson, H. W.; Bheda, M. C.; Engen, P. T. *Prog. Polym. Sci.* **1994**, *19*, 843. Gibson, H. W. In *Large Ring Molecules*; J. Wiley: New York, 1996; pp 191–262. (b) Gong, C.; Gibson, H. W. In *Molecular Catenanes, Rotaxanes and Knots*; Sauvage, J.-P.; Dietrich-Buchecker, C. O., Eds.; Wiley-VCH: Weinheim, 1999; pp 277–321. (c) Mahan, E.; Gibson, H. W. In *Large Ring Molecules*, 2nd ed.; Semlyen, J. A., Ed.; Kluwer: Dordrecht, 2000; pp 415–560.
- (a) Harada, A. *Adv. Polym. Sci.* **1997**, *133*, 141. (b) Ooya, T.; Yui, N. *Crit. Rev. Ther. Drug Carrier Syst.* **1999**, *16*, 289. (c) Raymo, F. M.; Stoddart, J. F. *Chem. Rev.* **1999**, *99*, 1643. (d) Harada, A. In *Materials Science and Technology, Synthesis of Polymers*; Schlüter, A.-D., Ed.; Wiley-VCH: Weinheim, 1999; Vol. 20, pp 485–512. (e) Takata, T.; Kihara, N. *Rev. Heteroat. Chem.* **2000**, *22*, 197. (f) Harada, A. *Acc. Chem. Res.* **2001**, *34*, 456. (g) Panova, I. G.; Topchieva, I. N. *Russ. Chem. Rev.* **2001**, *70*, 23.
- Gong, C.; Ji, Q.; Glass, T. E.; Gibson, H. W. *Macromolecules* **1997**, *30*, 4807.
- Gibson, H. W.; Liu, S.; Gong, C.; Ji, Q.; Joseph, E. *Macromolecules* **1997**, *30*, 3711.
- Gong, C.; Gibson, H. W. *Macromolecules* **1996**, *29*, 7029.
- Mason, P. E.; Bryant, W. S.; Gibson, H. W. *Macromolecules* **1999**, *32*, 1559.
- Mason, P. E.; Parsons, I. W.; Tolley, M. S. *Polymer* **1998**, *39*, 3981.
- Hodge, P.; Monvisade, P.; Owen, G. J.; Heatley, F.; Pang, Y. *New J. Chem.* **2000**, *24*, 703.
- Amabilino, D. B.; Anelli, P.-L.; Ashton, P. R.; Brown, G. R.; Cordova, E.; Godinez, L. A.; Hayes, W.; Kaifer, A. E.; Philp, D.; Slawin, A. M. Z.; Spencer, N.; Stoddart, J. F.; Tolley, M. S.; Williams, D. J. *J. Am. Chem. Soc.* **1995**, *117*, 11142.
- Wu, C.; Bheda, M. C.; Lim, C.; Shen, Y. X.; Sze, J.; Gibson, H. W. *Polym. Commun.* **1991**, *32*, 204.
- Gibson, H. W.; Engen, P. T.; Shen, Y. X.; Sze, J.; Lim, C.; Bheda, M.; Wu, C. *Makromol. Chem. Macromol. Symp.* **1992**, *54/55*, 519.
- Gibson, H. W.; Marand, H. *Adv. Mater.* **1993**, *5*, 11.
- Shen, Y. X.; Xie, D.; Gibson, H. W. *J. Am. Chem. Soc.* **1994**, *116*, 537.
- Morris, K. F.; Johnson Jr., C. S. *J. Am. Chem. Soc.* **1993**, *115*, 4291.
- Schulze, D.; Stilbs, P. *J. Magn. Reson. A* **1993**, *105*, 54.
- Persson, K.; Griffiths, P. C.; Stilbs, P. *Polymer* **1996**, *37*, 253.
- Jerschow, A.; Müller, N. *Macromolecules* **1998**, *31*, 6573.
- Håkansson, B.; Nydén, M.; Söderman, O. *Colloid Polym. Sci.* **2000**, *278*, 399.
- Skinner, P. J.; Blair, S.; Katakay, R.; Parker, D. *New J. Chem.* **2000**, *24*, 265.
- Cameron, K. S.; Fielding, L. *J. Org. Chem.* **2001**, *66*, 6891.
- Gafni, A.; Cohen, Y. *J. Org. Chem.* **1997**, *62*, 120.
- Avram, L.; Cohen, Y. *J. Org. Chem.* **2002**, *67*, 2639.
- Gibson, H. W.; Bheda, M. C.; Engen, P.; Shen, Y. X.; Sze, J.; Zhang, H.; Gibson, M. D.; Delaviz, Y.; Lee, S.-H.; Liu, S.; Wang, L.; Nagvekar, D.; Rancourt, J.; Taylor, L. T. *J. Org. Chem.* **1994**, *59*, 2186.
- Gibson, H. W.; Engen, P. T.; Lee, S.-H. *Polymer* **1999**, *40*, 1823.
- Wu, D.; Chen, A.; Johnson Jr., C. S. *J. Magn. Reson. A* **1995**, *115*, 260.
- (a) Nakashima, Y. *Am. Mineral.* **2001**, *86*, 132. (b) Mills, R. *J. Phys. Chem.* **1973**, *77*, 685.
- Provencher, S. W. *Comput. Phys. Commun.* **1982**, *27*, 213.
- Provencher, S. W. *Comput. Phys. Commun.* **1992**, *229*. CONTIN is available at <http://s-provencher.com/pages/contin.shtml>.
- (a) Callaghan, P. T.; Pinder, D. N. *Macromolecules* **1981**, *14*, 1334. (b) *Polymer Handbook*, 4th ed.; Brandrup, J.; Immergut, E. H., Grulke, E. A., Eds.; John Wiley & Sons: New York, 1999.
- (a) Johnson Jr., C. S. *Prog. Nucl. Magn. Reson. Spectrosc.* **1999**, *34*, 203. (b) Pelta, M.; Barjat, H.; Morris, G. A.; Davis, A. L.; Hammond, S. J. *Magn. Reson. Chem.* **1998**, *36*, 706.
- Antalek, B. *Concepts Magn. Reson.* **2002**, *14*, 225.
- Harris, R. K.; Kinnear, K. A.; Morris, G. A.; Stchedroff, M. J.; Samadi-Maybodi, A.; Azizi, N. *Chem. Commun.* **2001**, 2422.
- (a) Beckham, H. W.; Nagapudi, K.; Girardeau, T.; Zhao, T.; Leisen, J. *Polym. Prepr.* **2003**, *44* (1), 263. (b) White, B.; Watson, W. P.; Beckham, H. W. *Polym. Prepr.* **2003**, *44* (1), 839.
- Jayawickrama, D. A.; Larive, C. K.; McCord, E. F.; Roe, D. C. *Magn. Reson. Chem.* **1998**, *36*, 755.
- Gong, C.; Ji, Q.; Subramaniam, C.; Gibson, H. W. *Macromolecules* **1998**, *31*, 1814.
- Gibson, H. W.; Bryant, W. S.; Lee, S.-H. *J. Polym. Sci., Part A: Polym. Chem.* **2001**, *39*, 1978.

MA025959G